



CFD analysis for ESO's extremely large telescope (ELT) in Chile: Wind screening performance of the dome and main structure

by Cimolai, ESO

The Extremely Large Telescope (ELT) is a 40m-class optical, near and mid-infrared telescope located at Cerro Amajones in the Chilean Andes about 150km south of the city of Antofagasta. Currently under construction, it will be the largest optical and infrared telescope in the world and will be operated and serviced by the ESO Paranal Observatory located approximately 20km away.

The design, manufacture, transport to site, assembly and testing of the ELT has been entrusted to the ACe consortium, led by the Italian company Cimolai. Success in this major engineering and technical challenge requires close cooperation between various technical and commercial departments, suppliers and workshops.

The telescope has an altitude-azimuth mount weighing approximately 4,700t housed in an enclosure called a dome and supported by a concrete base. The telescope itself comprises a rotating steel structure (the main structure, MS) that integrates numerous subsystems, including the optics, electronics, and controls.

In summary, the ELT consists of the following main components: concrete dome foundation and pier; auxiliary dome building; rotating part of the dome; concrete MS foundation and pier; rotating MS structure. The MS consists of a steel space-frame structure with a highly optimized rotating mass that simultaneously guarantees the dynamic requirements and system-level performance (including pointing stability and tracking capability).

To meet the performance requirements across the entire observation field, the telescope structure must be adequately protected from the action of the wind. Indeed, due to its large size, the mirrors and

hosted units (HU) are susceptible to wind effects that can affect the accuracy of observations.

A retractable windscreen (WS) was thus implemented to protect the mirrors and hosted units from gusts of wind by controlling the flow entering the dome chamber. The ELT windscreen has four porous aluminium panels, each with a span of 42m and a height of 10m, that can be fully deployed or retracted depending on the elevation of the main structure. Each is designed with a minimum permeability of 20% (ratio of perforated area to total area), necessary for thermal performance as it promotes air recirculation within the telescope to improve thermal homogeneity within the dome chamber during

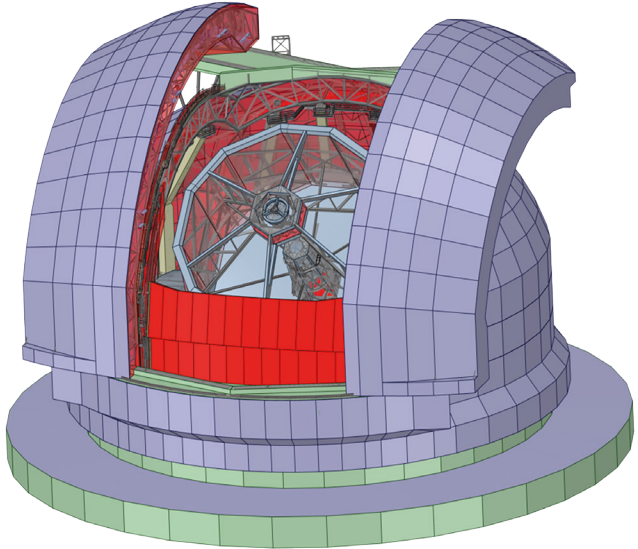


Fig. 1. Non-simplified DMS geometry.

observation. Thermal behaviour is, in fact, a crucial aspect of the main structure's performance.

A CFD (computational fluid dynamics) analysis was carried out to evaluate the windscreen's performance in controlling wind velocity in the vicinity of the mirrors and the hosted units under typical environmental conditions and to test different types of porous panels. Today, CFD has become common practice in the industrial process of civil structures as it provides an in-depth view of the flow field.

However, the geometric complexity of the dome and main structure (DMS) system (Fig. 1) does not support simplified modelling but requires an intense effort to condense the geometric and aerodynamic characteristics using a methodical, subsystem-based approach. This work was conducted by extensively using the concept of porous volumes, i.e. fluid volumes capable of representing specific aerodynamic properties of the real system.

Specifically, the characterization of the porous media representing the windscreen was performed in three steps: first, the CFD model of the panel, with explicitly modelled holes, was validated against experimental data obtained from wind tunnel tests (WTT) performed in previous design phases. Second, a porous numerical model of two different porous panel geometries one flat (OP) and one corrugated (CP), was characterized to provide the same pressure drop and deflection angles as the models with explicitly modelled holes, but with a reasonable computational effort.

Finally, a benchmark validation of the free flow was performed to demonstrate the effectiveness of the porous model in a real flow. A similar characterization was performed for the lattice structures inside the dome, which did not require explicit modelling. The porous models were then introduced into the overall CFD model, thereby enabling the calculation of the flow field inside the dome chamber for various angles of attack of the wind.

Modelling approach

Model objectives

A CFD model was constructed with the aim of determining the mean field of motion near the M1, M2 and M4 mirrors to verify the performance requirements of the windscreen, which were formulated in terms of the maximum permissible velocity in a series of specific probes, shown in Fig. 2:

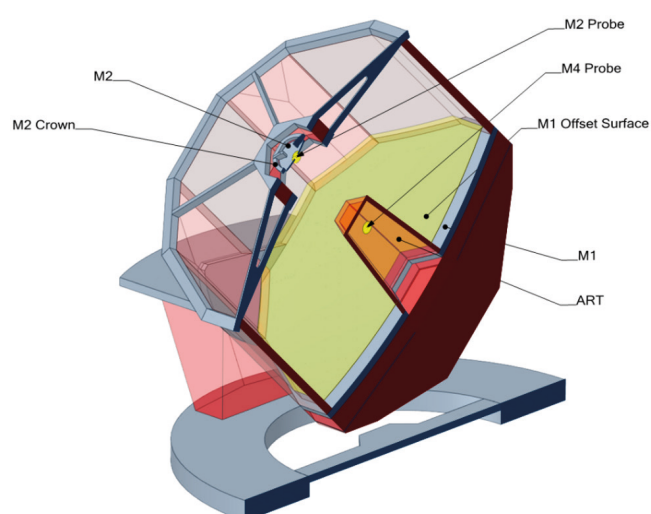


Fig. 2. Probe locations.

- Probes M2 and M4 positioned at the vertices of mirrors M2 and M4, respectively.
- M1 offset surface provides spatially continuous data interpolated from the values of the nearest cell node.
- M1 mean is calculated as a weighted average (facet area) over the entire offset surface.
- M1 max is the maximum (spatial) value on the offset surface.

The analysis was performed for different load cases (LC), different altitude positions and wind attack angles (Fig. 3):

- LC-AZ0-(20 | 60 | 90 | 180)-ALT45: altitude 45° and azimuth 0°, 20°, 60°, 90°, 180°, respectively, to evaluate performance in typical conditions.
- LC-WT-AZ0-ALT90: altitude 90° and azimuth 0°, considered to validate the model with the wind tunnel test.

In the two elevation configurations, the windscreen panels are correspondingly unfolded and modelled as independent bodies, allowing the airflow in the interstices to be simulated.

Sub-system decomposition

The ELT geometry is extraordinarily complex due to the large number of lattice truss structures and highly detailed components that may or may not affect the flow within the dome chamber. The introduction of porous media (Fig. 4) was necessary because such a highly detailed 3D CFD computational grid cannot be handled using reasonable

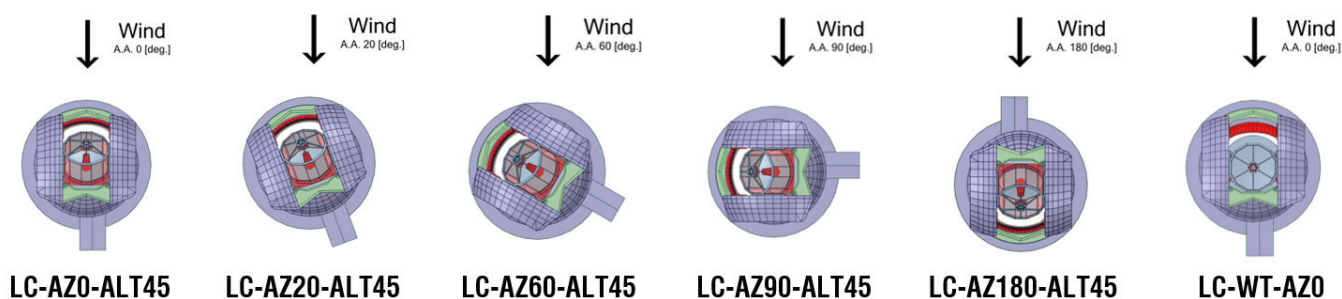


Fig. 3. Load cases.

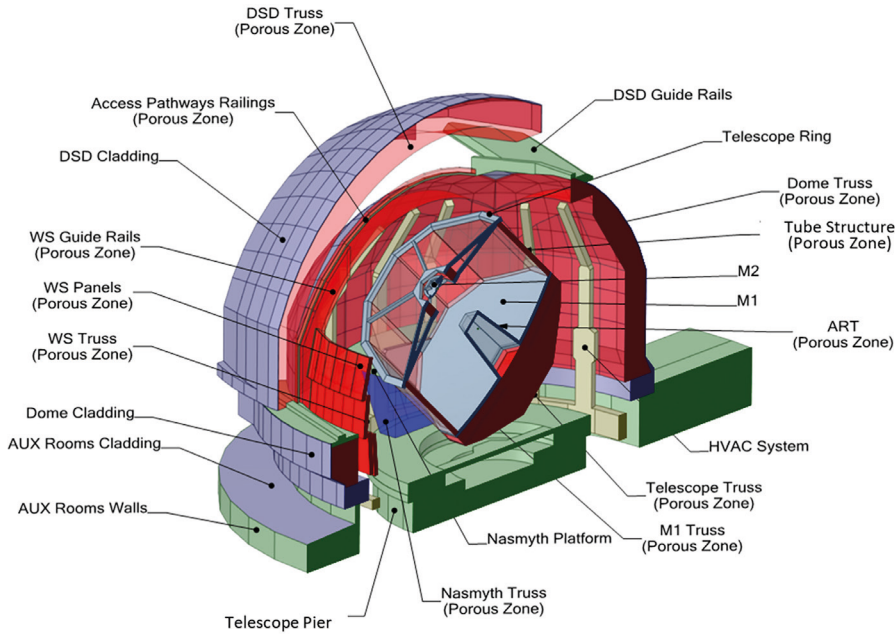


Fig. 4. ELT geometry and section.

computational resources. Porous zones are fluid volumes that enable the passage of air while offering the same resistance to flow as a real body but with a significantly reduced number of cells.

Numerically, this is accomplished by introducing a “sink” term in the Navier-Stokes equation that must be properly calculated. Given its primary importance in the aerodynamic behaviour of the structure, specific CFD tests were performed on the windscreen panel to correctly calibrate the porous media in terms of pressure loss and deflection angle.

Further CFD studies were conducted to estimate the pressure loss coefficients of other elements that are considered to affect the wind flow in the Hosted Units, such as the dome truss and dome sliding doors

(DSD) truss; the windscreen truss, the tube structure and the adaptive relay tower (ART) structure. Less detailed porous media were also used for other complex truss structures that have a marginal influence on the flow field. In these cases, an analytical fine-tuning of the porous parameters was conducted.

Porous media modelling Windscreen

Each windscreen panel consists of two porous zones: a thin high-resistance zone representing the perforated panels and a thicker lower-resistance zone representing the truss structure (Fig. 5).

Special care was required to develop accurate porous modelling of the thin perforated panel because it had to provide a realistic aerodynamic response for the actual panel both in terms of pressure loss and flow deflection. The porous model of the

perforated windscreen panel was developed in three stages:

- Validation of the CFD model of the perforated panel with explicitly modelled holes against wind tunnel data.
- Calculation of the porous model parameters providing the same pressure drop and deflection angles as the explicit CFD models of the perforated panel in two panel geometries, flat (OP) and corrugated (CP).
- Benchmarking the performance of the porous model for a finite-sized panel immersed in free flow.

Truss structures

Lattice structures are very numerous within the DMS. However, they play a minor role in influencing the flow field within the dome chamber, which is mainly driven by the outer cladding and the windscreen. Therefore, their effect was reproduced macroscopically through porous media (Fig. 6).

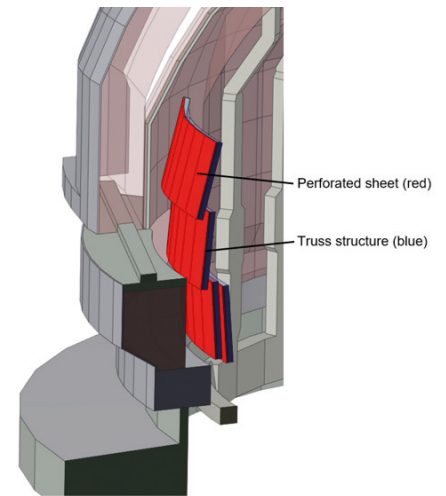


Fig. 5. Representation of porous windscreen.

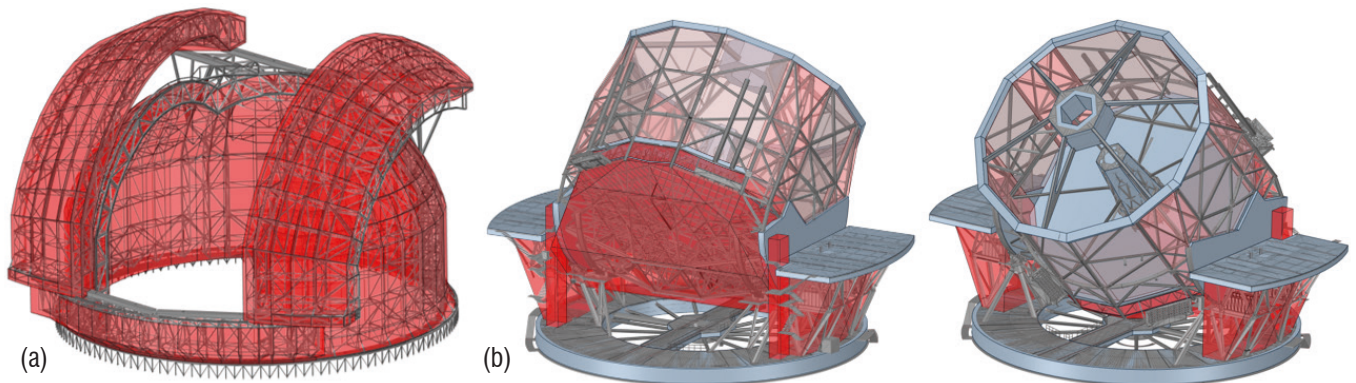


Fig. 6. Porous zones (red) of the dome and DSD and, b) of the main structures.

Pressure loss coefficients were defined using both an analytical and a CFD approach.

Overall CFD model

Model configuration

The purpose of this model is to determine time-averaged information for specific areas of the DMS structure, so a steady state RANS (Reynolds-Averaged Navier-Stokes) simulation was performed using Ansys Fluent software. The RANS equations are derived from the instantaneous Navier-Stokes equations using Reynolds decomposition, whereby an instantaneous quantity is decomposed into its time-averaged and fluctuating parts. Thus RANS equations include an apparent stress term (Reynolds stress), which originates from the fluctuating part of the non-linear acceleration terms and is solved using turbulence models.

In RANS methods, the entire turbulence spectrum is modelled and only the mean flow is resolved. RANS models have been remarkably successful in providing the industry with sufficient and reasonably accurate design information and are considered an industry standard. In this work, the Realizable $k-\epsilon$ Turbulence Model was used with the Ansys Fluent Scalable Wall Treatment.

Steady-state simulations were performed on a scaled model using the same geometric scale as the one used in the wind tunnel tests (1:70) to allow validation of the results. The boundary conditions applied to the overall model are summarized in Table 1.

Boundary	Velocity	Pressure	Turbulence Characteristics
Inlet	ABL	$\partial p/\partial x=0$	ABL
Outlet	$\partial U/\partial x=0$	ABL Outlet	Zero Gradient
Ground	$U=0$	$\partial p/\partial x=0$	Zero Gradient
Sky	Symmetry B.C	Symmetry B.C	Symmetry B.C
Left/Right	Symmetry B.C	Symmetry B.C	Symmetry B.C

Table 1. Overall model boundary conditions.

A correct ABL configuration at the inlet is essential to obtain meaningful results from a CFD study. Moreover, the inlet wind velocity profile and turbulence model variables (turbulent kinetic energy and viscous dissipation) were calculated so that the resulting wind profile at the telescope location are close to the requested environmental conditions. The roughness of the terrain was also set to allow the turbulence intensity to persist through the domain.

Mesh sensitivity

To check the numerical uncertainty, several simulations were performed with different grids showing that the simulation results were grid-independent. A grid independence study was performed to assess the best level of refinement of the grid (Fig. 7). Furthermore, an appropriate refinement was performed with approximately ten layers of inflation at the walls leading to y^+ between 30 and 300.

The lower limit cannot be met for many surfaces within the dome due to the extremely low wind speeds. This has little impact on the

solution as it is reasonable to expect that the velocity and pressure fields inside the dome depend only marginally on the behaviour of the inner wall. Nevertheless, Fluent’s Scalable Wall Functions were used so that viscous regions could be modelled correctly in these situations. Since the windscreen is modelled as a porous volume it does not function as a wall and therefore y^+ cannot be defined for it.

Different model geometry assumptions were tested to assess the influence of the grid on the flow field at the probes, as shown in Table 2.

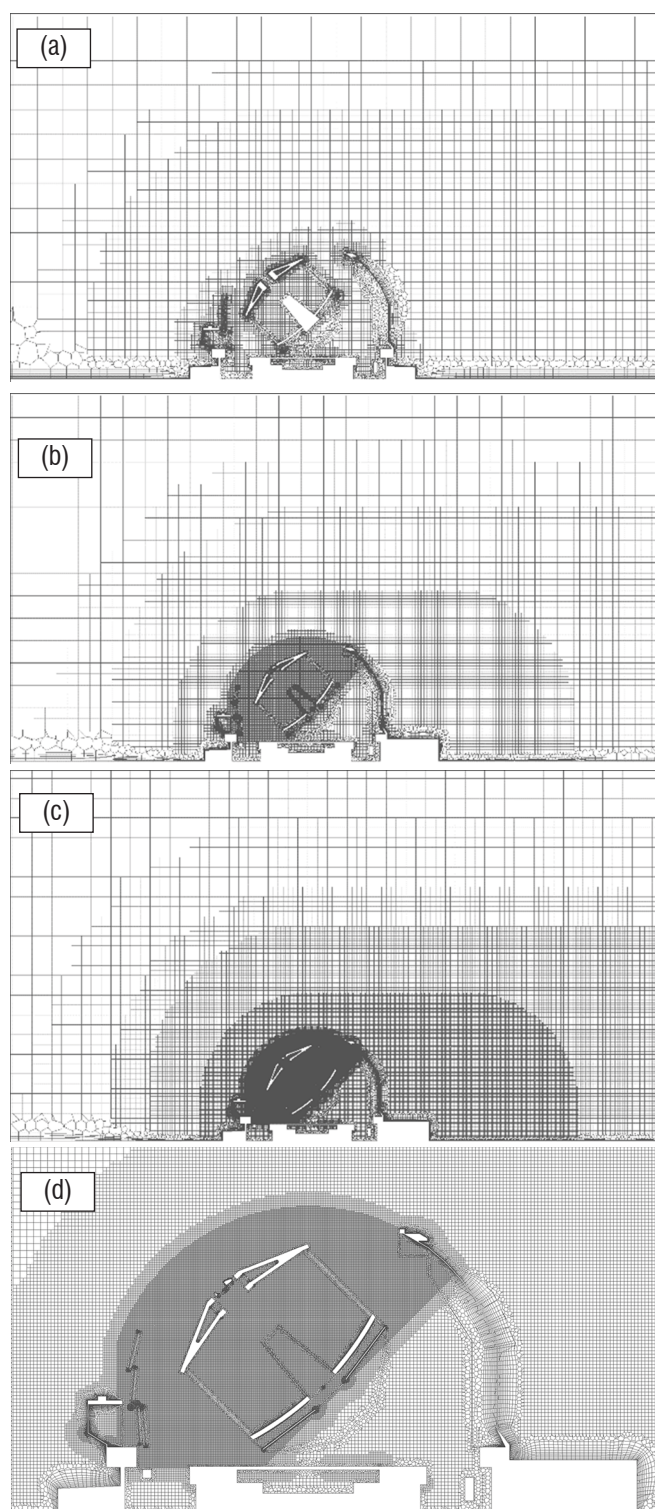


Fig. 7. Different levels of mesh: a) coarse, b) medium, c) fine, d) detail of fine mesh.

Mesh #	#of Cells	M1 mean	M1 max	M2 probe	M4 probe	Note
1	$8 \cdot 10^6$	$0.85V_{ref.1}$	$1.16V_{ref.2}$	$0.92 V_{ref.3}$	-	Coarse Mesh
2	$24 \cdot 10^6$	$1.05V_{ref.1}$	$1.68V_{ref.2}$	$0.85 V_{ref.3}$	-	Medium Mesh
3	$24 \cdot 10^6$	$1.01V_{ref.1}$	$0.99V_{ref.2}$	$1.00V_{ref.3}$	$1.01V_{ref.4}$	Same as 2. Porous ART and M2 are introduced
4	$24 \cdot 10^6$	$1.00V_{ref.1}$	$1.00V_{ref.2}$	$1.00V_{ref.3}$	$1.03V_{ref.4}$	Same as 3. Internal mesh inflation layer is introduced.
5	$40 \cdot 10^6$	$1.01V_{ref.1}$	$1.00V_{ref.2}$	$1.00V_{ref.3}$	$1.10V_{ref.4}$	Geometry same as 4. Model is in full scale (1:1)
6	$50 \cdot 10^6$	$V_{ref.1}$	$V_{ref.2}$	$V_{ref.3}$	$V_{ref.4}$	Fine mesh. Geometry and inflation layer settings the same as in 4.

Table 2. Mesh sensitivity results for LC-AZO.

A full-scale simulation was also performed which demonstrated the independence of the result from the Reynolds number. Based on the results, mesh refinement grade 4 (Medium) was used for the complete calculations.

Results

This section shows a selection of representative results of the analyses in configurations LC-AZO-ALT45, LC-AZ90-ALT45, and LC-WT-AZO.

LC-AZO-ALT45

In this load case the windscreen's performance is crucial as the incoming wind encounters no other obstacles. Fig. 8b shows the effect of the windscreen on the velocity field.

LC-AZ90-ALT45

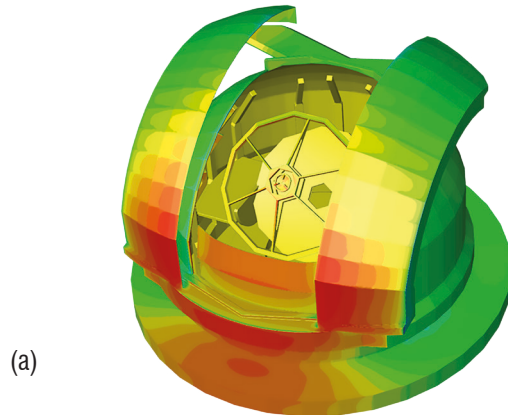
In this load case, the opening is almost completely shielded by the DSD and dome cladding. The M2 mirror lies in the full slipstream of the cladding. The windscreen here has less effect on the flow field than in LC-AZO-ALT45, however, some flow still enters through the observation slit in the slipstream of the dome cladding (Fig. 9).

LC-WT-AZO

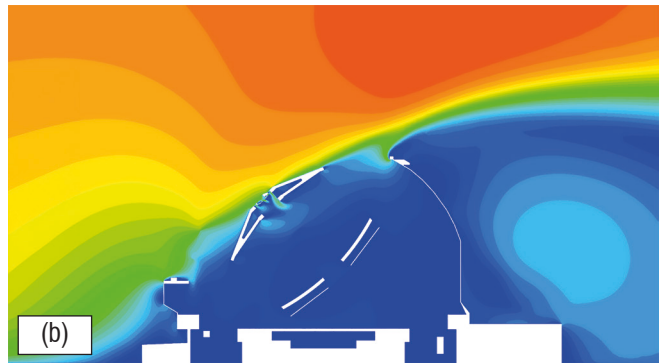
This simulation was performed specifically to validate the model's ability to accurately estimate speeds at the hosted units. It was quantified by comparing the results of case LC-AZO-ALT90 against measurements in the wind tunnel test at the same probe locations. The wind tunnel model represents a comparable situation in terms of boundary conditions and elevation angle of the telescope.

Point	V WTT [m/s]	V CFD WS OP [m/s]	V CFD WS:CP [m/s]
P1	7.75	7.21	7.23
P2	2.81	2.92	3.08
M1-Top	0.31	0.34	0.38
M1-Centre	0.20	0.10	0.12
M1-Right	0.32	0.38	0.31
M1-Left	0.11	0.38	0.31
M1-Bottom	0.32	0.05	0.08
M2	4.26	4.84	4.88
M4	0.58	0.96	1.08

Table 3. Velocity comparison between the WTT and CFD.



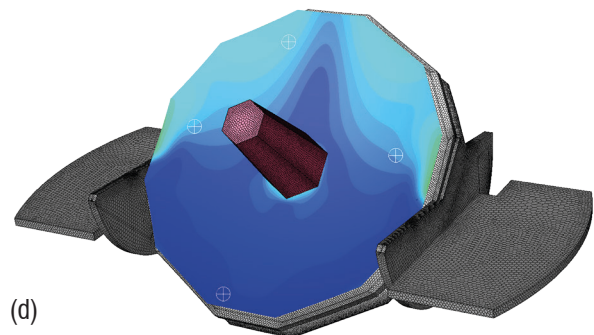
(a)



(b)



(c)



(d)

Fig. 8. Pressure contours: a) overall, b) orthogonal plane: velocity contours, c) longitudinal plane, d) M1.

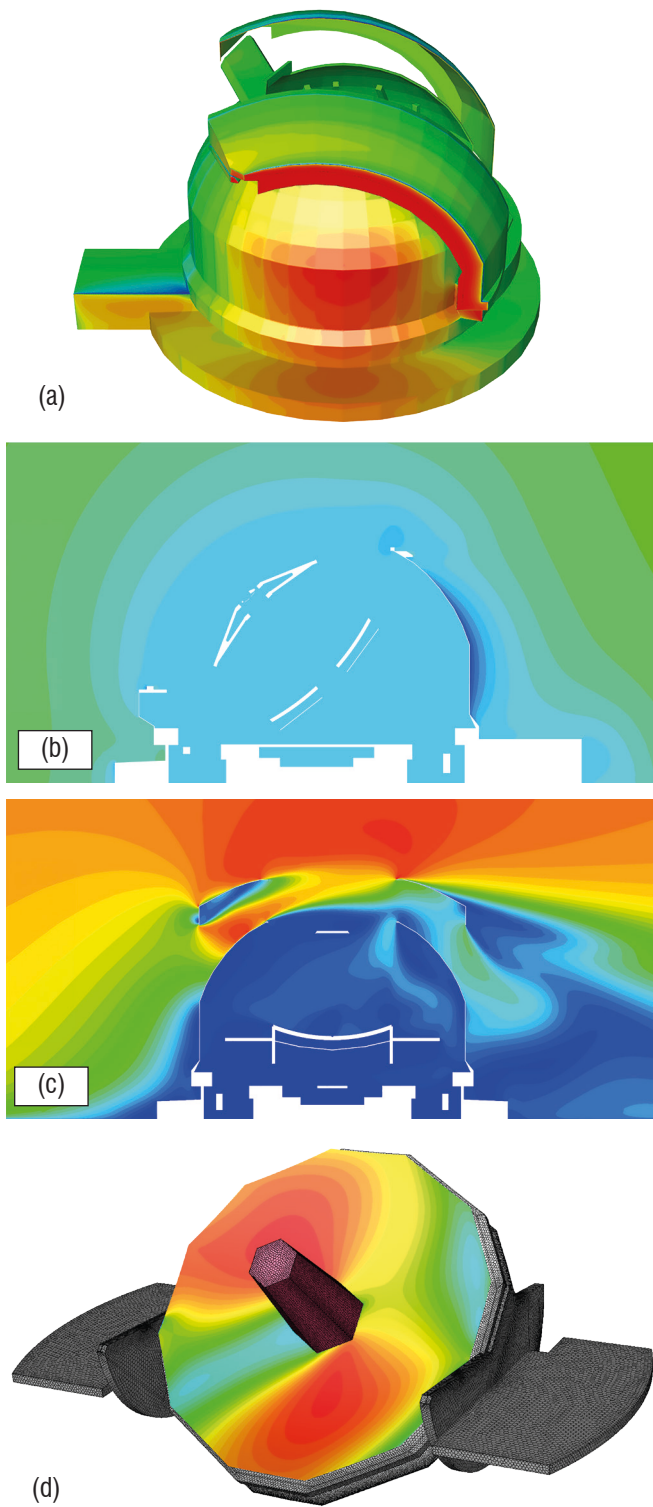


Fig. 9. Pressure contours: a) overall, b) orthogonal plane: velocity contours, c) longitudinal plane, d) M1.

The results obtained from the CFD calculation in terms of the velocity measured on the probes, shown in Fig. 10, are very close to those obtained in the wind tunnel test. The position of the probes on M1 is shown in Fig. 10c; the probe on M2 and on M4 is positioned according to Fig. 2.

The results of this analysis confirm the validity of the study presented here, particularly concerning speed measurements in the vicinity of the mirrors, which is the main focus of the study.

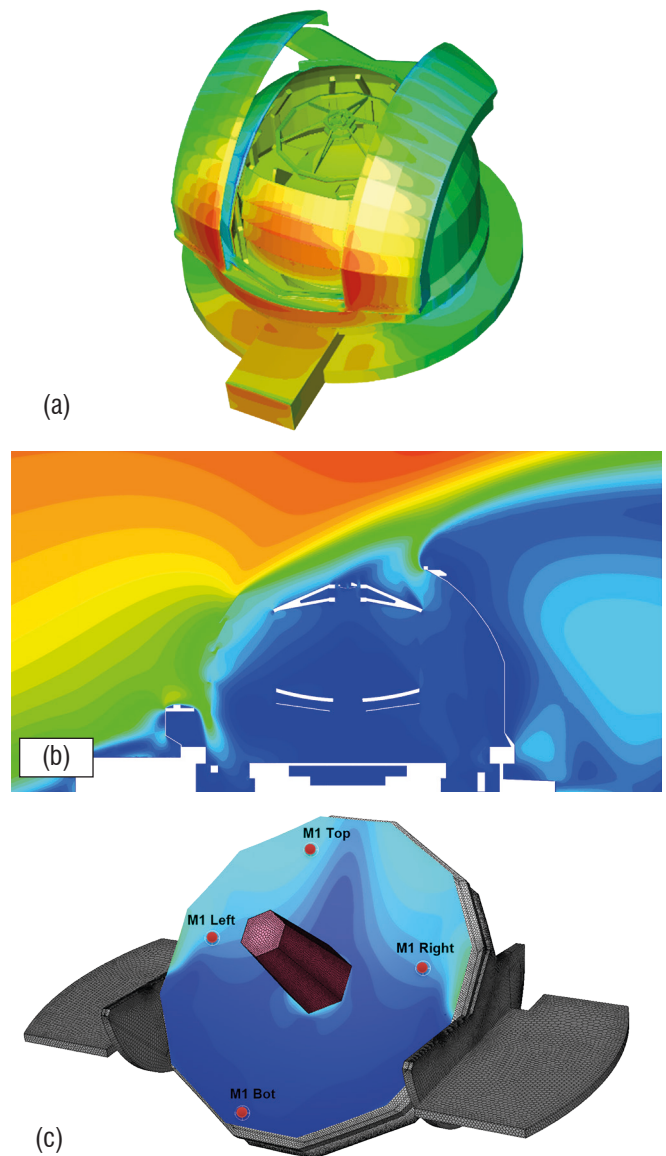


Fig. 10. Pressure contours: a) overall, b) orthogonal plane: velocity contours, c) M1.

The wind tunnel test results were also validated in terms of both local and integral pressures.

Effects on hosted units

The windscreen's performance was measured by the CFD model in terms of velocities near the M1, M2 and M4 mirrors.

The simulations resulted in the following values for both the flat perforated sheet (OP) and the corrugated perforated sheet (CP). Only the results for Azimuths 0° and 90° are shown here.

Velocity [m/s]	OP		CP	
	0°	90°	0°	90°
M1 mean	0.17	1.20	0.16	1.15
M1 max	0.45	1.60	0.45	1.60
M2	4.84	0.30	4.88	0.38
M4	0.38	0.40	0.44	0.40

Table 4. WS performance - OP and CP.

These results demonstrate the windscreen's effectiveness in shielding from external wind during observation. Both designs (OP and CP) result in remarkably similar velocity values at the mirrors and represent a viable solution for windscreen performance.

Currently, the CP design is preferred from a structural point of view. It is also thermodynamically preferred due to its lower permeability as it provides better flow recirculation.

Conclusions

The CFD analysis was performed following the ESO Technical Specifications and demonstrated the windscreen's effectiveness in shielding the Hosted Units from the wind. First, the geometric model for the CFD simulation was created at a scale of 1:70 based on wind tunnel assumptions and considering suitably simplified geometric characteristics; porous regions were inserted in place of truss structures.

The windscreen was also modelled as a porous region. Given the windscreen's importance in internal wind flow behaviour, the porous windscreen model was rigorously analysed and the porous model parameters were identified.

The performance of the porous windscreen model was also compared with both wind tunnel tests and high-fidelity CFD simulations, yielding satisfactory results in terms of pressure drop, deflection angle, resultant forces, nearby velocity field and nearby pressure field.

Auxiliary CFD studies were performed to obtain the properties of other porous regions that replaced various truss structures. The boundary conditions were set to meet the requirements of the specifications on velocity profiles and turbulence intensity level. These conditions were tested on an empty domain, demonstrating good persistence of the above-mentioned characteristics throughout the domain.

Several sensitivity studies were performed to determine the sensitivity of the model to both mesh size and other model assumptions such as geometry, scale, roughness, etc. In total five load cases were considered with varying angles of attack for the 45° altitude configuration. In addition, a 90° altitude configuration with the windscreen fully extended was considered as a benchmark test. The benchmark tests showed good agreement with the wind tunnel tests.

This CFD model also serves other purposes beyond calculating the windscreen performance. It is part of the numerical chain to calculate convective heat exchanges in the night-time thermal analysis of the Main Structure. This is crucial to assess the main structure's thermal deflections during the observational part of its thermal analysis. In that simulation, the model also considers the effect of the louvers.

This study allowed us to understand the characteristics of wind flow within the dome under typical observational conditions and to demonstrate the windscreen's adequacy in protecting the telescope from the effect of the wind in order to allow observation tasks.

About Cimolai

Cimolai is a leading metal construction company based in Italy. It has been engaged in the design, manufacture, and erection of complex steel structures for over 70 years. Over time, Cimolai has diversified its activities in the field of industrial, civil, military, naval and oil and gas engineering. It also operates in the field of curtain walling, special cladding and oversized element handling systems. The company has been entrusted with iconic projects around the world, including the planet's largest telescope, the ELT (Extremely Large Telescope) in Chile; Calatrava's "Oculus" underground station at Ground Zero in New York; the Vessel honeycomb structure in the Hudson Yards complex in Manhattan in New York; the new Pilot Tower in Genoa in Italy; lot 2 of Line 17 of the Paris Metro; the new Fiumicino Airport Terminal in Italy; the new railway station in Sesto San Giovanni in Milan in Italy; and the Al Wasl Plaza Dome for the 2020 World Expo in Dubai. For more information, visit: cimolai.com

About ESO

The European Southern Observatory (ESO) enables scientists worldwide to discover the secrets of the Universe for the benefit of all. It designs, builds, and operates world-class observatories on the ground and promotes international collaboration for astronomy. Established as an intergovernmental organization in 1962, today ESO is supported by 16 member states (Austria, Belgium, Czechia, Denmark, France, Finland, Germany, Ireland, Italy, the Netherlands, Poland, Portugal, Spain, Sweden, Switzerland, and the United Kingdom), the host state of Chile, and Australia as a strategic partner. ESO's headquarters and its visitor centre and planetarium, the ESO Supernova, are located close to Munich in Germany, while the Chilean Atacama Desert hosts the telescopes. ESO operates three observing sites: La Silla, Paranal and Chajnantor. At Paranal, ESO operates the Very Large Telescope and its Very Large Telescope Interferometer, as well as survey telescopes such as VISTA. At Paranal ESO will also host and operate the Cherenkov Telescope Array South, the world's largest and most sensitive gamma-ray observatory. Together with international partners, ESO operates ALMA on Chajnantor, a facility that observes the skies in the millimetre and submillimetre ranges. At Cerro Armazones, near Paranal, it is building "the world's biggest eye on the sky" — ESO's Extremely Large Telescope. It supports its operations in the country and engages with Chilean partners and society from its offices in Santiago in Chile.

For more information:
media@cimolai.com